

Defect Melting of Vortices in High-T_c Superconductors

Jürgen Dietel and Hagen Kleinert

Institut für Theoretische Physik, Freie Universität Berlin, Arnimallee 14, D-14195 Berlin, Germany

(Dated: Received February 16, 2019)

We set up a melting model for vortex lattices in high-temperature superconductors based on the continuum elasticity theory. The model is Gaussian and includes defect fluctuations by means of a discrete-valued vortex gauge field. We derive the melting temperature of the lattice and predict the size of the Lindemann number. Our result agrees well with experiments for YBa₂Cu₃O_{7-δ}, and with modifications also for Bi₂Sr₂CaCu₂O₈. We calculate the jumps in the entropy and the magnetic induction at the melting transition.

PACS numbers: 74.25.Qt, 74.72.-h

The magnetic flux lattices in high-temperature superconductors can undergo a melting transition suggested by Nelson in 1988 [1]. The detailed properties of this transition have been studied in many theoretical and experimental papers. The simplest estimates for the transition temperature came from an adaption of the famous Lindemann criterion of three-dimensional ordinary crystals [2]. The adaption is due to Houghton et al. and Brandt [3], and states that the vortex lattice undergoes a melting transition once the mean thermal displacement $\langle u^2 \rangle^{1/2}$ becomes a certain fraction of the lattice spacing $a \approx (\Phi_0/B)^{1/2}$, where Φ_0 is the flux quantum and B the magnetic induction. The ratio $c_L \equiv \langle u^2 \rangle^{1/2}/a$ is the characteristic Lindemann number, which should be independent of B . Its value is *not* predicted by Lindemann's criterion. It must be extracted from experiments, and is usually found in the range $c_L \approx 0.1 - 0.3$. The most prominent examples of high-temperature superconductors which exhibit vortex lattice melting are the anisotropic compound YBa₂Cu₃O_{7-δ} (YBCO), and the strongly layered compound Bi₂Sr₂CaCu₂O₈ (BSCCO). Decoration experiments on BSCCO [4] show the formation of a triangular vortex lattice, neutron scattering on YBCO of a tilted square lattice of vortices [5] close to the melting region, the latter being favored by the *d*-wave symmetry of the order parameter and the anisotropy of the crystal [6]. An explicit calculation of the Lindemann number $c_L = \langle u^2 \rangle^{1/2}/a$ for YBCO can be found in Ref. 3 and for BSCCO in Ref. 7.

In this letter, we present a theory which is capable of specifying the size of the Lindemann number c_L . Basis is a simple Gaussian model which takes into account both lattice elasticity and defect degrees of freedom in the simplest possible way. The relevance of defect fluctuations to understanding the melting transition is well-known. For ordinary crystals, this is textbook material [2]. In the context of vortex melting it was emphasized in Ref. [8]. For ordinary crystals, the size of the Lindemann number has been calculated successfully by means of Gaussian lattice models with elastic and defect fluctuations, which clearly display first-order melting transitions in three dimensions and both first-order or sequence of continuous transitions in two dimensions.

An important quality of these models is that in the

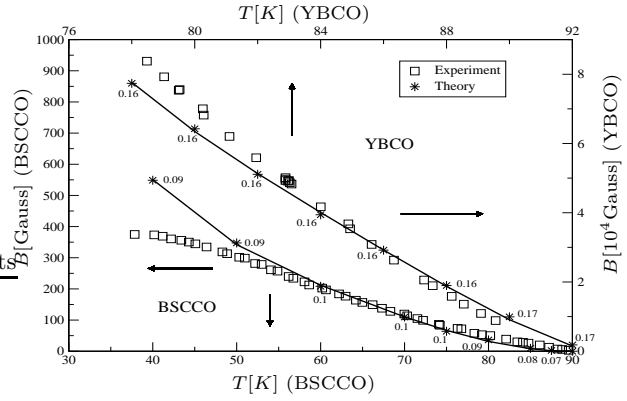


FIG. 1: Melting curve $B = B_m(T)$ for YBCO and BSCCO. The experimental values are from Ref. 17 for YBCO and Ref. 16 for BSCCO. The numbers on the theoretical melting curves are the Lindemann numbers c_L calculated from (9).

first-order case, where fluctuations are small, they lead to a simple universal melting formula determining the melting point in terms of the elastic constants. The universal result is found from a lowest-order approximation, in which one identifies the melting point with the intersection of the high-temperature expansion of the free energy density dominated by defect fluctuations with the low-temperature expansion dominated by elastic fluctuations. The resulting universal formula for the melting temperature determines also the size of the Lindemann number. In two dimensions, this procedure was recently generalized from square to triangular lattices [9]. A similar intersection criterium was also used for the melting point of vortex lattices in the Abrikosov approximation of the Ginzburg-Landau model [10] useful for YBCO. Here we shall apply our defect model to calculate the melting curve of the vortex lattices in YBCO and BSCCO.

Due to the large penetration depth λ_{ab} in the layers in comparison to a we have to take into account the full non-local elasticity constants when integrating over the Fourier space, as emphasized by Brandt in Ref. 11. For our Gaussian model, the partition function of the vortex lattice can be split into $Z = Z_0 Z_{\text{fl}}$ where Z_0 is the partition function of the rigid lattice and Z_{fl} is thermally fluctuating part calculated via the elastic Hamiltonian plus defects. Due to the translational invariance of the vor-

tex lattice in the direction of the vortices, which we shall take to be the z -axis, we may simply extend the models on square [2] and triangular lattices [9] by a third dimension along the z -axis, which we artificially discretize to have a lattice spacing a_3 , whose value will be fixed later. The elastic energy is

$$E_{\text{el}} = \frac{v}{2} \sum_{\mathbf{x}} (\nabla_i u_i) (c_{11} - 2c_{66}) (\nabla_i u_i) + \frac{1}{2} (\nabla_i u_j + \nabla_j u_i) c_{66} (\nabla_i u_j + \nabla_j u_i) + (\partial_z u_i) c_{44} (\partial_z u_i). \quad (1)$$

The subscripts i, j (l, m, n) have values 1, 2 (1, ..., 3), the vectors $u_i(\mathbf{x})$ are given by the transverse displacements of the line elements of the vortex lines with coordinate \mathbf{x} . We have suppressed the spatial arguments of the elasticity parameters, which are really functional matrices $c_{ij}(\mathbf{x}, \mathbf{x}') \equiv c_{ij}(\mathbf{x} - \mathbf{x}')$. Their precise forms were calculated by Brandt [11]. The volume of the fundamental cell v is equal to $a^2 a_3$ (square) or $a^2 a_3 \sqrt{3}/2$ (triangular). For a square lattice, the lattice derivative ∇_i in (1) are given by $\nabla_i f(\mathbf{x}) = [f(\mathbf{x} + a\mathbf{e}_i) - f(\mathbf{x})]/a$

and $\nabla_3 f(\mathbf{x}) = [f(\mathbf{x} + a_3 \mathbf{e}_3) - f(\mathbf{x})]/a_3$. For a triangular lattice, the xy -part of the lattice has the link vectors $\pm a \mathbf{e}_{(m)}$ with $\mathbf{e}_{(1,3)} = (\cos 2\pi/6, \pm \sin 2\pi/6, 0)$ and $\mathbf{e}_{(2)} = (-1, 0, 0)$. The lattice derivatives around a plaquette are defined by $\nabla_{(1)} f(\mathbf{x}) = [f(\mathbf{x} + a\mathbf{e}_{(1)}) - f(\mathbf{x})]/a$, $\nabla_{(2)} f(\mathbf{x}) = [f(\mathbf{x}) - f(\mathbf{x} - a\mathbf{e}_{(2)})]/a$, $\nabla_{(3)} f(\mathbf{x}) = [f(\mathbf{x} - a\mathbf{e}_{(2)}) - f(\mathbf{x} + a\mathbf{e}_{(1)})]/a$. From these we define discrete cartesian lattice derivatives used in the Hamiltonian (1) $\nabla_i f(\mathbf{x}) = (2/3)e_{(l)} \nabla_{(l)} f(\mathbf{x})$ and $\nabla_3 f(\mathbf{x}) = [f(\mathbf{x} + a_3 \mathbf{e}_3) - f(\mathbf{x})]/a_3$ transforming like the continuum derivative with respect to the symmetry group of the lattice [9]. Therefore, the Hamiltonian (1) has the full symmetry of the triangular lattice and the correct continuum elastic energy for zero lattice spacing.

Within the elastic approximation the displacement fields are restricted to values within the fundamental cell. In order to contain also defect degrees of freedoms one has to insert into (1) integer valued defect gauge fields [2]. In the canonical stress representation, the partition function containing these fields becomes

$$Z_{\text{fl}} = \det \left[\frac{c_{66}}{4(c_{11} - c_{66})} \right]^{1/2} \det \left[\frac{1}{2\pi\beta} \right]^{5/2} \prod_{\mathbf{x}} \left[\prod_{i \leq m} \int_{-\infty}^{\infty} d\sigma_{im} \right] \left[\prod_m \sum_{n_m(\mathbf{x})=-\infty}^{\infty} \right] \left[\int_{-\infty}^{\infty} \frac{d\mathbf{u}}{a} \right] \exp \left\{ - \sum_{\mathbf{x}} \frac{1}{2\beta} \times \left[\sum_{i < j} \sigma_{ij}^2 + \frac{1}{2} \sum_i \sigma_{ii}^2 - \left(\sum_i \sigma_{ii} \right) \frac{c_{11} - 2c_{66}}{4(c_{11} - c_{66})} \left(\sum_i \sigma_{ii} \right) + \sum_i \sigma_{i3} \frac{c_{66}}{c_{44}} \sigma_{i3} \right] \right\} e^{2\pi i \sum_{\mathbf{x}} (\sum_{i \leq m} \nabla_m u_i \sigma_{im} + \sum_{i < j} D_{ij} \sigma_{ij})}. \quad (2)$$

The parameter β is given by $\beta = v c_{66} / k_B T (2\pi)^2$. σ_{ij} represent stress fields [2]. The matrix $D_{ij}(\mathbf{x})$ in Eq. (2) is a discrete-valued local defect matrix composed of integer-valued defect gauge fields n_1, n_2, n_3 for square [2] and triangular vortex lattices [9] as follows:

$$D_{ij}^{\square} = \begin{pmatrix} n_1 & n_3 \\ n_3 & n_2 \end{pmatrix}, \quad (3)$$

$$D_{ij}^{\triangle} = \begin{pmatrix} \frac{1}{2}n_1 & \frac{1}{\sqrt{3}}(n_1 - n_2) + \frac{2}{\sqrt{3}}n_3 \\ \frac{1}{\sqrt{3}}(n_1 - n_2) + \frac{2}{\sqrt{3}}n_3 & -\frac{1}{2}n_1 - n_2 \end{pmatrix}. \quad (4)$$

The vortex gauge fields specify the *Volterra surfaces* in units of the Burgers vectors. By summing over all $n_{1,2,3}(\mathbf{x})$, the partition function Z_{fl} includes all defect fluctuations, dislocations as well as disclinations. There is a constraint for a vortex lattice which does not exist for ordinary three-dimensional lattices. Dislocations in the vortex lattice can be both screw or edge type, but in either case the defect lines are confined in the plane spanned by their Burger's vector and the magnetic field [8, 12]. The reason is that the flux lines in a vortex lattice cannot be broken. This results in the constraint $D_{11} = -D_{22}$ on the defect fields.

We now calculate the low-temperature expansion of the partition function Z_{fl} to lowest order, which includes only the $n_m = 0$ -term. By carrying out the integration over the displacement fields $u_i(\mathbf{x})$ in (2) we obtain, as in [2, 9], the leading term in the low-temperature expansion of the free energy

$$Z_{\text{fl}}^{T \rightarrow 0} = \left(\frac{a_3}{a} \right)^{2N} \frac{1}{\det [(2\pi\beta)c_{44}/c_{66}]} e^{-N \sum_{i \in \{1,6\}} l_{ii}}, \quad (5)$$

where

$$l_{ii} = \frac{1}{2} \frac{1}{V_{\text{BZ}}} \int_{\text{BZ}} d^2 k dk_3 \log \left[\frac{c_{ii} a_3^2}{c_{44}} K_j^* K_j + a_3^2 K_3^* K_3 \right]. \quad (6)$$

Here K_m is the eigenvalue of $i\nabla_m$. The momentum integrations in (6) run over the Brioullin zone of the vortex lattice whose volume is $V_{\text{BZ}} = (2\pi)^3/v$, as indicated by the subscript BZ.

Next we calculate the high-temperature expansion $Z_{\text{fl}}^{T \rightarrow \infty}$ to lowest order. By carrying out the integration over the displacement fields $u_i(\mathbf{x})$ in (2) and further by summing over the defect fields n_m under the considera-

tion $D_{11} = -D_{22}$ mentioned above we obtain

$$Z_{\text{fl}}^{T \rightarrow \infty} = \left(\frac{a_3}{a}\right)^{2N} \frac{C^N}{2^N \det[(2\pi\beta)^2 c_{44}/c_{66}]} e^{-Nh} \quad (7)$$

with

$$h = \frac{1}{2} \frac{1}{V_{\text{BZ}}} \int_{\text{BZ}} d^2 k dk_3 \log \left[1 + \frac{c_{11} - c_{66}}{c_{44}} \frac{K_j^* K_j}{K_3^* K_3} \right]. \quad (8)$$

The constant C has the values $C_{\square} = 1$ for the square vortex lattice and $C_{\triangle} = \sqrt{3}$ for the triangular one.

From the partition function (2) with no defects ($n_m = 0$) we obtain for the Lindemann number $c_L = \langle u^2 \rangle^{1/2}/a$ the momentum integral

$$c_L^2 = \frac{a_3^2}{a^2 v} \frac{k_B T}{V_{\text{BZ}}} \int_{\text{BZ}} d^2 k dk_3 \frac{1}{c_{44}} \sum_{i=1,6} \frac{1}{\frac{c_{ii} a_3^2}{c_{44}} K_j^* K_j + a_3^2 K_3^* K_3}. \quad (9)$$

This can be simplified by taking into account that c_{11} is much larger than c_{66}, c_{44} [11]. As announced, we find the melting temperature from the intersection of low- and high-temperature expansions, obtained by equating $Z_{\text{fl}}^{T \rightarrow 0} = Z_{\text{fl}}^{T \rightarrow \infty}$. By taking into account $\det[a_3^2 \nabla_3^* \nabla_3] = 1$ we obtain $h, l_{11} \ll l_{66}$, and further that the $i = 1$ -term in (9) is much smaller than the $i = 6$ -term. In the following analytic discussion (but not in the numerical plots) we neglect these small contributions. The temperature of melting is then given by the simple formula

$$\frac{k_B T}{v} \frac{1}{\det^{1/N}[c_{66}]} C = \frac{e^{-l_{66}}}{\pi}, \quad (10)$$

where $\det[c_{66}]$ is the determinant of the $N \times N$ functional matrix c_{66} . The elastic moduli c_{44} and c_{66} at low reduced magnetic fields $b \equiv B/H_{c2} < 0.25$ can be taken from Brandt's paper [11]

$$c_{66} = \frac{B\phi_0\zeta}{(8\pi\lambda_{ab})^2}, \quad (11)$$

$$c_{44} = \frac{B^2}{4\pi(1+\lambda_c^2 k^2 + \lambda_{ab}^2 k_3^2)} + \frac{B\phi_0}{32\pi^2 \lambda_c^2} \ln \frac{1 + \frac{2\lambda_c^2}{\langle u \rangle^2} + \lambda_{ab}^2 k_3^2}{1 + \lambda_c^2 K_{\text{BZ}} + \lambda_{ab}^2 k_3^2} + \frac{B\phi_0}{32\pi^2 \lambda_{ab}^4 k_3^2} \ln \frac{1 + \lambda_{ab}^2 k_3^2 / (1 + \lambda_{ab}^2 K_{\text{BZ}}^2)}{1 + \lambda_{ab}^2 k_3^2 / (1 + 2\lambda_{ab}^2 / \langle u \rangle^2)} \quad (12)$$

where λ_c is the penetration depth in the xy -plane, $\zeta = 1$, and K_{BZ} is the boundary of the circular Brillouin zone $K_{\text{BZ}}^2 = 4\pi B/\phi_0$. At high fields ($b > 0.5$), c_{66} is altered by a factor $\zeta \approx 0.71(1-b)$, and the penetration depths in c_{66}, c_{44} are replaced by $\tilde{\lambda}^2 = \lambda^2/(1-b)$, where λ denotes either λ_{ab} or λ_c . In addition, the last two terms in c_{44} are replaced by $B\phi_0/16\pi^2 \tilde{\lambda}_c^2$. For YBCO we have [13] $\lambda(T) = \lambda(0)[1 - (T/T_c)]^{-1/3}$, $\xi(T) = \xi(0)[1 - (T/T_c)]^{-1/2}$ for BSCCO [14] $\lambda(T) = \lambda(0)[1 - (T/T_c)^4]^{-1/2}$, $\xi(T) = \xi(0)[1 - (T/T_c)^4]^{-1/2}$. When calculating c_{44} in (12) we have used a momentum cutoff in the two-vortex interaction potential $k \leq 2/\langle u^2 \rangle^{1/2}$, and not the inverse of the correlation length $1/\xi$ as in Ref. 11. The cutoff is

due to thermal softening [2], and becomes relevant for $\langle u^2 \rangle^{1/2}/\xi \gg 1$, or equivalently for $c_L \sqrt{2\pi} \sqrt{H_{c2}(T)/B} \gg 1$, which is fulfilled in the melting regime of BSCCO, but not for YBCO.

It remains to determine the effective lattice spacing a_3 along the vortex lines. An elementary defect in the vortex lattice (arising for example from a crossing of two vortex strings) takes place over a typical length scale in the z -direction determined from the condition that the sum of elastic displacement energy and the energy required to stretch the line against the line tension is minimal. The energy of an ensemble of dislocations is determined by the interplay of elastic energy of small displacements and integer-valued defect fields. The relevant part of the free energy is given by the discretized free energy $-\log(Z_0 Z_{\text{fl}}) k_B T$ (2) in which a_3 is equal to the above length scale in the z -direction. To determine this, we insert the variational ansatz for the transverse displacement field $u_i = \delta_{i,1} A_0 \exp[-2|z|/a_3]$ into the continuum version (in z direction) of the elastic energy (1) and approximate $-\nabla_2^2 \approx \langle K_2^2 \rangle \approx K_{\text{BZ}}^2/4$ in E_{el} and $K^2 \approx \langle K^2 \rangle \approx K_{\text{BZ}}^2/2$ in the elastic constants, where the average $\langle \dots \rangle$ was taken with respect to a circular Brillouin zone. The optimal length scale a_3 is chosen such that E_{el} is minimal for a fixed amplitude $A_0 \approx a$ corresponding to a typical defect elongation.

In the following, we treat first the more isotropic square vortex crystal YBCO ($a = \sqrt{\phi_0/B}$). From c_{66} and c_{44} for YBCO, the optimal length scale is given by $a_3 = 4a\lambda_{ab}/\lambda_c\zeta(1-b)^{1/2}$. When comparing the melting criterium of the defect model in Eq. (10) with the Lindemann criterium obtained by equating the parameter (9) to a universal number, we obtain identical results when taking into account that the integrand in (9) and in l_{66} of Eq. (6) receive their main contribution from the region $k \approx \sqrt{\langle k^2 \rangle} \approx K_{\text{BZ}}/\sqrt{2}$. We can approximate $k_3 \approx 0$ in this region, resulting in $a_3^2 c_{66}/a^2 c_{44} \approx 4/\pi$. With the same approximation in Eqs. (6) and (9), we can perform the integrals numerically. Then we obtain from the melting condition (10) precisely the Lindemann criterium in which the Lindemann number (9) is predicted to be

$$\frac{k_B T_m}{4 \left[c_{44} \left(\frac{K_{\text{BZ}}}{\sqrt{2}}, 0 \right) c_{66} \left(\frac{K_{\text{BZ}}}{\sqrt{2}}, 0 \right) \right]^{1/2} a^3} \approx c_L^2 \approx (0.18)^2. \quad (13)$$

Denoting the spacing between the CuO_2 double layers by a_s we obtain for the entropy jump per double layer and vortex

$$\Delta S_l \approx k_B T_m (\partial/\partial T_m) (a_s/a_3) \ln[Z_{\text{fl}}^{T \rightarrow \infty}/Z_{\text{fl}}^{T \rightarrow 0}]. \quad (14)$$

Inserting (5) and (7), this becomes

$$\Delta S_l \approx \frac{k_B T_m a_s}{a_3} \frac{\partial}{\partial T_m} \ln \frac{k_B T_m / a^3}{\left[c_{44} \left(\frac{K_{\text{BZ}}}{\sqrt{2}}, 0 \right) c_{66} \left(\frac{K_{\text{BZ}}}{\sqrt{2}}, 0 \right) \right]^{1/2}}. \quad (15)$$

Finally, we make use of the Clausius-Clapeyron equation which relates the jump of the entropy density across the

melting transition to the jump of the magnetic induction by $\Delta S_l a_3 / v a_s = -(dH_m/dT) \Delta B / 4\pi$. Here H_m is the external magnetic field on the melting line. Combining the Clausius-Clapeyron equation with Eqs. (12) and (15) we obtain, with the abbreviation $\tau_m \equiv T_m/T_c$, the following relations near T_c :

$$\begin{aligned} B_m(T) &\approx \frac{12\zeta}{16^2\pi^4} \frac{(1-T/T_c)^{4/3} c_L^4 \phi_0^5}{(k_B T)^2 \lambda_{ab}^2(0) \lambda_c^2(0)}, \\ \Delta S_l &\approx \frac{\sqrt{\zeta} a_s}{6a} \frac{\lambda_c}{\lambda_{ab}(1-\tau_m)} \approx \frac{2.7}{10^3} \frac{a_s c_L^2 \phi_0^2}{T_c (1-\tau_m)^{1/3} \lambda_{ab}^2(0)}, \\ \Delta B &\approx \frac{\sqrt{\zeta} \pi}{2a \phi_0} \frac{\lambda_c}{\lambda_{ab}} T_m \approx \frac{2.5}{10^2} \frac{(1-\tau_m)^{2/3} c_L^2 \phi_0}{\lambda_{ab}^2(0)}. \end{aligned} \quad (16)$$

These results agree with the general scaling results in Ref. [15], with the advantage that here the prefactors are predicted whereas those in [15] had to be determined by fits to experimental curves (there is only a slight discrepancy because we use a different temperature dependence of the penetration depth).

Next, we calculate the corresponding expressions in the case of the more layered crystal BSCCO ($a = (2^{1/2}/3^{1/4})\sqrt{\phi_0/B}$). First, we have to determine the dislocation length scale a_3 in this case. For dislocation moves we have $\langle u^2 \rangle^{1/2} \sim 1/K_{BZ}$. This means that we can neglect the last two terms of c_{44} in (12), coming from the self-energy of the vortex line, when determining a_3 . Remembering this we obtain by a similar procedure as for YBCO the dislocation length scale $a_3 \approx 4a\sqrt{2}\lambda_{ab}/\lambda_c\sqrt{\pi}$. From this we find $a_3^2 c_{66}/a^2 c_{44} \ll 1$, resulting in $l_{66} \approx 0$. By taking into account that $B\pi^3\lambda_{ab}^2/32\phi_0 \lesssim 1$ on the melting line we obtain that $c_{44}(k, k_3)$ for $|k_3| < \pi/a_3$ is dominated by the last term in (12). Then we obtain

$$\begin{aligned} c_{44}(k, k_3) &\approx \frac{B\phi_0}{32\pi^2\lambda_{ab}^2(1+\lambda_{ab}^2 K_{BZ}^2)} \text{ for } k_3 \ll \frac{1}{\lambda_{ab}}, \quad (17) \\ c_{44}(k, k_3) &\approx \frac{B\phi_0 \ln(1+2B\lambda_{ab}^2/\phi_0 c_L^2)}{32\pi^2\lambda_{ab}^4 k_3^2} \text{ for } k_3 \gg \frac{1}{\lambda_{ab}}. \end{aligned}$$

By using these values we obtain by numerical integration of (9)

$$\begin{aligned} c_L^2 &\approx \frac{k_B T_m \cdot 0.36}{a^3 \sqrt{c_{66}(\frac{K_{BZ}}{\sqrt{2}}, 0) c_{44}(\frac{K_{BZ}}{\sqrt{2}}, 0)}} + \frac{k_B T_m a_3 \cdot 1.60}{a^4 c_{44}(\frac{K_{BZ}}{\sqrt{2}}, 1/a_3)} \\ &\approx \frac{k_B T_m \lambda_{ab}^2 \cdot 138}{\phi_0^2 a} \sqrt{1 + \lambda_{ab}^2 K_{BZ}^2} + \frac{k_B T_m \lambda_{ab}^2 \lambda_c^2 \cdot 137 \lambda_{ab}}{\phi_0^2 a^3 \log(1/c_L^2)} \frac{\lambda_{ab}}{\lambda_c} \end{aligned} \quad (18)$$

The first term comes from the integration region $|k_3| < 1/\lambda_{ab}$, the second from the region $1/\lambda_{ab} < |k_3| < \pi/a_3$ in (9).

From our melting criterion (10) and the Clausius-Clapeyron equation (where $dH_m/dT \approx dB_m/dT$ due to

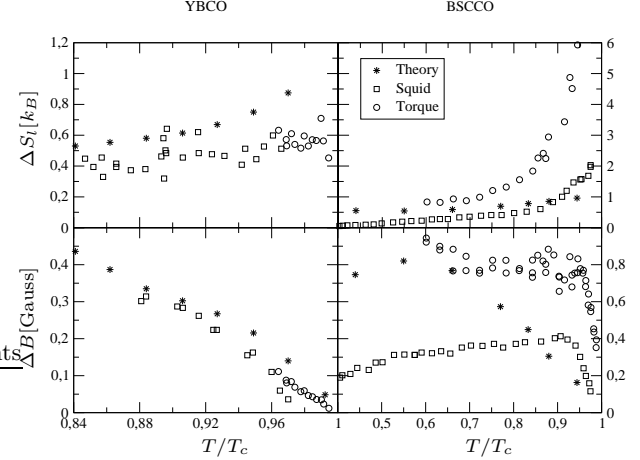


FIG. 2: Entropy jump per double layer per vortex ΔS_l (first row) and jump of magnetic induction field ΔB (second row) at the melting transition. The experimental values for YBCO are from Ref. 17 for ΔS_l , Ref. 18 for ΔB by squid experiments, and Ref. 19 by torque measurements. The experimental values for BSCCO are from Ref. 16 (squid) and Ref. 20 (torque).

$B_m(T) \gtrsim H_{c1}(T)$ [16]), we obtain for BSCCO

$$\begin{aligned} B_m(T) &\approx \frac{1}{192} \frac{1}{\sqrt{3}\pi^7} \frac{(1-(T/T_c)^4)^2}{\lambda_{ac}^2(0)\lambda_c^2(0)} \frac{\phi_0^5}{(k_B T)^2}, \\ \Delta S_l &\approx \frac{\sqrt{\pi} a_s k_B}{4\sqrt{2}a} \frac{\lambda_c}{\lambda_{ab}} \frac{1+3\tau_m^4}{1-\tau_m^4} \approx \frac{2.9}{10^4} \frac{a_s(1+3\tau_m^4)\phi_0^2}{T_m \lambda_{ab}^2(0)}, \\ \Delta B &\approx \frac{\pi^{3/2}}{2\sqrt{2}a} \frac{\lambda_c}{\lambda_{ab}} k_B T_m \approx \frac{1.8}{10^3} \frac{(1-\tau_m^4)\phi_0}{\lambda_{ab}^2(0)}. \end{aligned} \quad (19)$$

Parameter values for optimal doped YBCO (BSCCO) are given by [13] $\lambda_{ab}(0) \approx 1186\text{\AA}$ ($\lambda_{ab}(0) \approx 2300\text{\AA}$), $\xi_{ab}(0) \approx 15\text{\AA}$ ($\xi_{ab}(0) \approx 30\text{\AA}$), the CuO_2 double layer spacing $a_s = 12\text{\AA}$ ($a_s = 14\text{\AA}$), $T_c = 92.7\text{K}$ ($T_c = 90\text{K}$) and the anisotropy parameter $\gamma = \lambda_c/\lambda_{ab} \approx 5$ ($\gamma \approx 200$).

We now calculate numerically the melting curves, the associated Lindemann parameter c_L , the entropy and the magnetic induction jumps ΔS_l and ΔB from the intersection criterium of the full low- and high-temperature expressions (5) and (7) without further approximations. The results are shown in Fig. 1 and Fig. 2. Our approximate analytic results (16) and (19) turn out to give practically the same curves. For comparisons, we show in both figures the experimental curves for YBCO of Ref. 17, 18, 19 and for BSCCO of Ref. 16, 20. The temperature dependence of the Lindemann parameter for BSCCO in Fig. 1 comes mainly from the second term in (18), having its largest variation near T_c . Our curves are in reasonable agreement with the experimental data except at the end point of the melting line at low temperatures and near $T \approx T_c$. It could have been anticipated that our vortex lattice model is not a good approximation in these regimes. At low temperature, the discrepancy comes mainly from Josephson decoupling of the

layers [21], most pronounced for the strongly anisotropic BSCCO superconductor, which leads also to large pinning effects [22]. Near $T \approx T_c$, our model does not include the increase of the entropy by thermal creation of

vortices in addition to the ones caused by the external magnetic field which form the lattice [23]. For YBCO, also order parameter fluctuations become important [24] which are ignored here.

[1] D. R. Nelson, Phys. Rev. Lett. **60**, 1973 (1988).

[2] H. Kleinert, *Gauge Fields in Condensed Matter*, Vol. II *Stresses and Defects*, World Scientific, Singapore, 1989. (readable online at www.physik.fu-berlin.de/~kleinert/re.html#b2)

[3] A. Houghton *et al.*, Phys. Rev. B **40**, 6763 (1989); E. H. Brandt, Phys. Rev. Lett. **63**, 1106 (1989).

[4] P. Kim *et al.*, Phys. Rev. Lett. **77**, 5118 (1996).

[5] B. Keimer *et al.*, Phys. Rev. Lett. **73**, 3459 (1994).

[6] H. Won and K. Maki, Phys. Rev. B **53**, 5927 (1996).

[7] G. Blatter, V. Geshkenbein, A. Larkin, and H. Norborg, Phys. Rev. B **54**, 73 (1996).

[8] M. C. Marchetti and D. R. Nelson, Phys. Rev. B **41**, 1910 (1990); J. Kierfeld and V. Vinokur, Phys. Rev. B **61**, R14928 (2000).

[9] J. Dietel and H. Kleinert, cond-mat/0508780.

[10] S. E. Hikami, A. Fujita, and A. I. Larkin, Phys. Rev. B **44**, 10400 (1991).

[11] E. H. Brandt, Rep. Prog. Phys. **58**, 1465 (1995).

[12] R. Labusch, Physics Letters **22**, 9 (1966).

[13] S. Kamal *et al.*, Phys. Rev. Lett. **73**, 1845 (1994).

[14] M. Tinkham, *Introduction to Superconductivity*, McGraw-Hill, New York, 1996.

[15] M. J. Dodgson *et al.*, Phys. Rev. Lett. **80**, 837 (1998).

[16] E. Zeldov *et al.*, Nature (London) **375**, 791 (1995).

[17] A. Schilling *et al.*, Nature (London) **382**, 791 (1996).

[18] U. Welp *et al.*, Phys. Rev. Lett. **76**, 4809 (1996).

[19] M. Willemin *et al.*, Phys. Rev. Lett. **81**, 4236 (1998).

[20] K. Kadowki and K. Kimura, Phys. Rev. B **57**, 11674 (1998).

[21] L. I. Glazman and A. E. Koshelev, Phys. Rev. B **43**, 2835 (1991).

[22] T. Blasius *et al.*, Phys. Rev. Lett. **82**, 4926 (1999).

[23] S. Ryu and D. Stroud, Phys. Rev. B **57**, 14476 (1998).

[24] V. L. Ginzburg, Fiz. Tverd. Tela **2**, 2031 (1960) [Sov. Phys. Solide State **2**, 1824 (1961)].